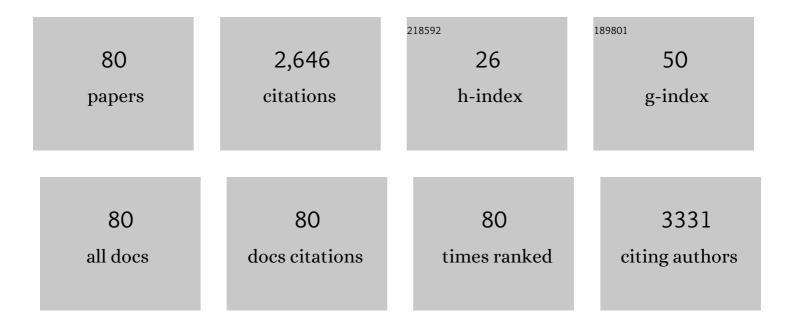
Xuanhong Cheng

List of Publications by Year in descending order

Source: https://exaly.com/author-pdf/5425985/publications.pdf Version: 2024-02-01



#	Article	IF	CITATIONS
1	Ultra-Wideband Impedance Spectroscopy of the Nucleus in a Live Cell. IEEE Journal of Electromagnetics, RF and Microwaves in Medicine and Biology, 2022, 6, 267-272.	2.3	4
2	Label-free focusing of viral particles under a temperature gradient coupled with continuous swirling flow. RSC Advances, 2022, 12, 4263-4275.	1.7	0
3	Effect of pulsatility on shearâ€induced extensional behavior of Von Willebrand factor. Artificial Organs, 2022, 46, 887-898.	1.0	10
4	Rare Event Prediction of Von Willebrand Factor Multimer Unfolding in Extensional Flow. Biophysical Journal, 2021, 120, 297a.	0.2	2
5	Predicting pathological von Willebrand factor unraveling in elongational flow. Biophysical Journal, 2021, 120, 1903-1915.	0.2	12
6	Recent Developments in Nanomaterialâ€Based Shearâ€5ensitive Drug Delivery Systems. Advanced Healthcare Materials, 2021, 10, e2002196.	3.9	24
7	Broadband electrical impedance as a novel characterization of oxidative stress in single L6 skeletal muscle cells. Analytica Chimica Acta, 2021, 1173, 338678.	2.6	5
8	Unraveling Kinetics of Collapsed Polymers in Extensional Flow. Macromolecules, 2021, 54, 8259-8269.	2.2	3
9	Flow-regulated nucleation protrusion theory for collapsed polymers. Physical Review E, 2021, 104, 054504.	0.8	1
10	Sensitivity Analysis for Ultra-Wideband 2-Port Impedance Spectroscopy of a Live Cell. IEEE Journal of Electromagnetics, RF and Microwaves in Medicine and Biology, 2020, 4, 37-44.	2.3	14
11	Broadband Electrical Sensing of a Live Biological Cell with In Situ Single-Connection Calibration. Sensors, 2020, 20, 3844.	2.1	5
12	Characterizing Single-Molecule Conformational Changes Under Shear Flow with Fluorescence Microscopy. Journal of Visualized Experiments, 2020, , .	0.2	1
13	Broadband Electrical Sensing of Nucleus Size in a Live Cell From 900 Hz to 40 GHz. , 2020, , .		5
14	Validation of Clausius–Mossotti Function in Wideband Single-Cell Dielectrophoresis. IEEE Journal of Electromagnetics, RF and Microwaves in Medicine and Biology, 2019, 3, 127-133.	2.3	12
15	Integration of Hierarchical Micro-/Nanostructures in a Microfluidic Chip for Efficient and Selective Isolation of Rare Tumor Cells. Micromachines, 2019, 10, 698.	1.4	3
16	Correlation Between Optical Fluorescence and Microwave Transmission During Single-Cell Electroporation. IEEE Transactions on Biomedical Engineering, 2019, 66, 2223-2230.	2.5	9
17	Broadband Scanning Microwave Microscopy of a Biological Cell with Unprecedented Image Quality and Signal-to-Noise Ratio. , 2019, , .		6
18	Editorial for the Special Issue on "Micro- and Nanofluidics for Bionanoparticle Analysis― Micromachines, 2019, 10, 600.	1.4	0

#	Article	IF	CITATIONS
19	A mechano-reactive coarse-grained model of the blood-clotting agent von Willebrand factor. Journal of Chemical Physics, 2019, 151, 124905.	1.2	13
20	Platelet mechanosensing axis revealed. Nature Materials, 2019, 18, 661-662.	13.3	3
21	Prediction of Sub-Monomer A2 Domain Dynamics of the von Willebrand Factor by Machine Learning Algorithm and Coarse-Grained Molecular Dynamics Simulation. Scientific Reports, 2019, 9, 9037.	1.6	2
22	Shear-Induced Extensional Response Behaviors of Tethered von Willebrand Factor. Biophysical Journal, 2019, 116, 2092-2102.	0.2	19
23	Tangential Flow Microfiltration for Viral Separation and Concentration. Micromachines, 2019, 10, 320.	1.4	7
24	Inverted scanning microwave microscope for <i>in vitro</i> imaging and characterization of biological cells. Applied Physics Letters, 2019, 114, .	1.5	20
25	Intensity-modulated nanoplasmonic interferometric sensor for MMP-9 detection. Lab on A Chip, 2019, 19, 1267-1276.	3.1	13
26	A Low-Cost, Point-of-Care Sickle Cell Anemia Screening Device for Use in Low and Middle-Income Countries. , 2019, , .		1
27	Quantitative Scanning Microwave Microscopy of the Evolution of a Live Biological Cell in a Physiological Buffer. IEEE Transactions on Microwave Theory and Techniques, 2019, 67, 5438-5445.	2.9	18
28	Ultra-wideband Electrical Sensing of Nucleus Size in a Live Cell. , 2019, , .		5
29	Transparency of PDMS based microfluidic devices under temperature gradients. Journal of Micromechanics and Microengineering, 2019, 29, 015014.	1.5	7
30	Coarse-Grain Modeling of Shear-Induced Binding between von Willebrand Factor and Collagen. Biophysical Journal, 2018, 114, 1816-1829.	0.2	11
31	Differentiation of live and heat-killed E. coli by microwave impedance spectroscopy. Sensors and Actuators B: Chemical, 2018, 255, 1614-1622.	4.0	41
32	Circular Nanoplasmonic Interferometer for Detection of Immune-Cell Secretion. , 2018, , .		0
33	Internal Tensile Force and A2 Domain Unfolding of von Willebrand Factor Multimers in Shear Flow. Biophysical Journal, 2018, 115, 1860-1871.	0.2	11
34	Ultra-wideband Characterization, Electroporation, and Dielectrophoresis of a Live Biological Cell Using the Same Vector Network Analyzer. , 2018, , .		7
35	Ultra-Wideband Impedance Spectroscopy of a Live Biological Cell. IEEE Transactions on Microwave Theory and Techniques, 2018, 66, 3690-3696.	2.9	39
36	Optimization of nanoparticle focusing by coupling thermophoresis and engineered vortex in a microfluidic channel. Journal of Applied Physics, 2017, 121, .	1.1	6

#	Article	IF	CITATIONS
37	Distributed Effect in High-Frequency Electroporation of Biological Cells. IEEE Transactions on Microwave Theory and Techniques, 2017, 65, 3503-3511.	2.9	34
38	Micropatterned macroporous structures in microfluidic devices for viral separation from whole blood. Analyst, The, 2017, 142, 2220-2228.	1.7	6
39	"Living―dynamics of filamentous bacteria on an adherent surface under hydrodynamic exposure. Biointerphases, 2017, 12, 02C410.	0.6	6
40	Influences of Adhesion Variability on the "Living―Dynamics of Filamentous Bacteria in Microfluidic Channels. Molecules, 2016, 21, 985.	1.7	8
41	Perfused drop microfluidic device for brain slice culture-based drug discovery. Biomedical Microdevices, 2016, 18, 46.	1.4	13
42	Investigation of Controllable Nanoscale Heat-Denatured Bovine Serum Albumin Films on Graphene. Langmuir, 2016, 32, 12623-12631.	1.6	14
43	Microfluidic devices with templated regular macroporous structures for HIV viral capture. Analyst, The, 2016, 141, 1669-1677.	1.7	6
44	Highly efficient and selective isolation of rare tumor cells using a microfluidic chip with wavy-herringbone micro-patterned surfaces. Analyst, The, 2016, 141, 2228-2237.	1.7	47
45	Enhancement of binding kinetics on affinity substrates by laser point heating induced transport. Analyst, The, 2016, 141, 1807-1813.	1.7	8
46	Flow-induced conformational change of von Willebrand Factor multimer: Results from a molecular mechanics informed model. Journal of Non-Newtonian Fluid Mechanics, 2015, 217, 58-67.	1.0	15
47	Assessment of Cytoplasm Conductivity by Nanosecond Pulsed Electric Fields. IEEE Transactions on Biomedical Engineering, 2015, 62, 1595-1603.	2.5	49
48	Maintenance and Neuronal Cell Differentiation of Neural Stem Cells C17.2 Correlated to Medium Availability Sets Design Criteria in Microfluidic Systems. PLoS ONE, 2014, 9, e109815.	1.1	21
49	Nanoporous anodic aluminum oxide with a long-range order and tunable cell sizes by phosphoric acid anodization on pre-patterned substrates. Electrochimica Acta, 2014, 117, 498-503.	2.6	28
50	Broadband Electrical Detection of Individual Biological Cells. IEEE Transactions on Microwave Theory and Techniques, 2014, 62, 1905-1911.	2.9	62
51	Measuring the Soret coefficient of nanoparticles in a dilute suspension. Journal of Nanoparticle Research, 2014, 16, 2625.	0.8	12
52	Gravity-induced swirl of nanoparticles in microfluidics. Journal of Nanoparticle Research, 2013, 15, 1611.	0.8	4
53	Plasmonic interferometric sensor arrays for high-performance label-free biomolecular detection. Lab on A Chip, 2013, 13, 4755.	3.1	89
54	Optofluidic Platform for Realâ€Time Monitoring of Live Cell Secretory Activities Using Fano Resonance in Gold Nanoslits. Small, 2013, 9, 3532-3540.	5.2	52

#	Article	IF	CITATIONS
55	Enumerating virus-like particles in an optically concentrated suspension by fluorescence correlation spectroscopy. Biomedical Optics Express, 2013, 4, 1646.	1.5	11
56	Plasmonic interferometers for label-free multiplexed sensing. Optics Express, 2013, 21, 5859.	1.7	55
57	Circular plasmonic interferometers for ultrasensitive low-background optical sensing. , 2013, , .		ο
58	Fabrication of Macroporous Polymeric Membranes through Binary Convective Deposition. ACS Applied Materials & Interfaces, 2012, 4, 4532-4540.	4.0	13
59	Emerging technologies for point-of-care CD4 T-lymphocyte counting. Trends in Biotechnology, 2012, 30, 45-54.	4.9	97
60	A microfabricated electrical differential counter for the selective enumeration of CD4+ T lymphocytes. Lab on A Chip, 2011, 11, 1437.	3.1	62
61	Effect of Surface Nanotopography on Immunoaffinity Cell Capture in Microfluidic Devices. Langmuir, 2011, 27, 11229-11237.	1.6	33
62	Plasmonic Mach–Zehnder Interferometer for Ultrasensitive On-Chip Biosensing. ACS Nano, 2011, 5, 9836-9844.	7.3	148
63	Microfluidic separation of viruses from blood cells based on intrinsic transport processes. Biomicrofluidics, 2011, 5, 32004-3200410.	1.2	13
64	Infrared light induced patterning of proteins on ppNIPAM thermoresponsive thin films: a "protein laser printer― Lab on A Chip, 2010, 10, 1079.	3.1	7
65	Micro- and nanotechnology for viral detection. Analytical and Bioanalytical Chemistry, 2009, 393, 487-501.	1.9	71
66	Enhancing the performance of a point-of-care CD4+ T-cell counting microchip through monocyte depletion for HIV/AIDS diagnostics. Lab on A Chip, 2009, 9, 1357.	3.1	102
67	Conjunctival Impression Cytology by Using a Thermosensitive Adhesive: Polymerized N-isopropyl Acrylamide. Cornea, 2009, 28, 770-773.	0.9	2
68	A REVERSIBLE THERMOSENSITIVE ADHESIVE FOR RETINAL IMPLANTS. Retina, 2008, 28, 1338-1343.	1.0	26
69	REVERSIBLE THERMOSENSITIVE GLUE FOR RETINAL IMPLANTS. Retina, 2007, 27, 938-942.	1.0	16
70	A microfluidic device for practical label-free CD4+ T cell counting of HIV-infected subjects. Lab on A Chip, 2007, 7, 170-178.	3.1	312
71	Cell detection and counting through cell lysate impedance spectroscopy in microfluidic devices. Lab on A Chip, 2007, 7, 746-755.	3.1	136
72	Comparison of Native Extracellular Matrix with Adsorbed Protein Films Using Secondary Ion Mass Spectrometry. Langmuir, 2007, 23, 50-56.	1.6	87

#	Article	IF	CITATIONS
73	Thermoresponsive MALDI Probe Surfaces as a Tool for Protein On-Probe Purification. Analytical Chemistry, 2007, 79, 6840-6844.	3.2	6
74	A Microchip Approach for Practical Label-Free CD4+ T-Cell Counting of HIV-Infected Subjects in Resource-Poor Settings. Journal of Acquired Immune Deficiency Syndromes (1999), 2007, 45, 257-261.	0.9	81
75	Temperature dependent activity and structure of adsorbed proteins on plasma polymerizedN-isopropyl acrylamide. Biointerphases, 2006, 1, 61-72.	0.6	83
76	A Plasma-Deposited Surface for Cell Sheet Engineering: Advantages over Mechanical Dissociation of Cells. Plasma Processes and Polymers, 2006, 3, 516-523.	1.6	34
77	Surface Characterization of the Extracellular Matrix Remaining after Cell Detachment from a Thermoresponsive Polymer. Langmuir, 2005, 21, 1949-1955.	1.6	156
78	Surface Chemical and Mechanical Properties of Plasma-Polymerized N-Isopropylacrylamide. Langmuir, 2005, 21, 7833-7841.	1.6	170
79	Novel cell patterning using microheater-controlled thermoresponsive plasma films. Journal of Biomedical Materials Research - Part A, 2004, 70A, 159-168.	2.1	112
80	Infrared Light Induced Patterning of Proteins on ppNIPAM Thermoresponsive Thin Films: A "Protein Laser Printer― , 0, , .		0